P-ISSN 2586-9000
E-ISSN 2586-9027
Homepage : *https://tci-thaijo.org/index.php/SciTechAsia* **Science & Technology Asia**
Vol. 29 No.3 July – September 2024 Page: [135-145]
Original research article

Molecular Interactions of Polyphenolic Compounds Binding on Antiapoptotic Wild-Type and Mutated Bcl-2 Proteins

Ayomi Vidana Pathiranage[1], Kulpavee Jitapunkul[2], Anotai Suksangpanomrung[3], Pisanu Toochinda[1], Luckhana Lawtrakul[1, *]

[1]*School of Bio-Chemical Engineering and Technology, Sirindhorn International Institute of Technology, Thammasat University, Pathum Thani 12120, Thailand*
[2]*Department of Chemical Engineering, Faculty of Engineering, Kasetsart University, Bangkok 10900, Thailand*
[3]*Department of Mechanical Engineering, Academic Division, Chulachomklao Royal Military Academy, Nakhon Nayok 26001, Thailand*

Received 7 December 2023; Received in revised form 10 July 2024
Accepted 1 August 2024; Available online 25 September 2024

ABSTRACT

The molecular docking approach was used to determine the binding affinities and the interactions of B-cell lymphoma 2 (Bcl-2) both of wild-type and mutated Bcl-2 (Gly101Val) in complex with five polyphenolic compounds which were reported to have biological activity in cancer therapy: Hesperetin, Quercetin, Cleomiscosin B, 5'-Methoxy-7'-epi-jatrorin A, and Procyanidin B2. The compounds were found to act as BH3-mimetics. They bind into the hydrophobic groove of BH3 motifs. Procyanidin B2 exhibited favorable binding free energies for both wild-type and mutated Bcl-2 (-8.30 to -8.80 kcal/mol). Molecular dynamics simulations and conformational analysis investigated the dynamics of Procyanidin B2 when bound to Bcl-2 in solution. Procyanidin B2 tightly binds to the hydrophobic groove of wild-type Bcl-2 (-24.79 kcal/mol) compared to the mutated species (-17.15 kcal/mol). Mutated residue in BH3 motifs induced structural changes, widening the hydrophobic cavity. This change potentially allows interference by surrounding water molecules, thereby weakening the protein-ligand interaction.

Keywords: BH3-mimetics; Computer-aided drug design; Conformational dynamics; Molecular docking; Molecular dynamics simulations

1. Introduction

From the early 1970s onward, cancer has consistently captivated the scientific community, sparking profound interest. This affliction persists as one of the most destructive diseases globally, claiming

***Corresponding author:** ayomi.vid@gmail.com **doi:** 10.14456/scitechasia.2024.51

millions of lives annually. As per the World Health Organization (WHO), cancer stands as a primary global cause of death, contributing to almost 10 million fatalities in 2020 [1], equivalent to nearly one in six deaths. They predicted the rising of cancer cases from 19.3 (2020) million to 30.2 million by 2040 [2]. Cancer cells exhibit several hallmarks, with evading apoptosis being a prominent feature. The primary cause of cancers, irrespective of their type, is the overexpression of antiapoptotic proteins [3]. The anti-apoptotic proteins are categorized under the B-Cell Lymphoma 2 (Bcl-2) family of proteins. The Bcl-2 family proteins regulate the intrinsic pathway, which is the key signaling pathway of apoptosis. The Bcl-2 family proteins regulate apoptosis by controlling mitochondrial outer membrane permeability through protein-protein interactions [4]. The unique feature of Bcl-2 family proteins is the presence of at least one Bcl-2 homology (BH) domain out of highly conserved four BH (BH1-BH4) regions [5]. Basis of the functional roles, Bcl-2 proteins are divided into pro-apoptotic, anti-apoptotic, and BH3-only proteins [4]. During apoptosis, BH3-only activators bind with both pro-apoptotic and antiapoptotic proteins [4]. BH3-only sensitizers release the BH3 activators from antiapoptotic proteins, which initiates mitochondrial outer membrane permeabilization, leading to the release of biomarkers, and triggering the activation of the apoptotis in a cell [6].

BH-3 mimetics are small molecules that can induce apoptosis in cancer cells by binding with antiapoptotic proteins [7]. Despite the creation of numerous BH3 mimetics, their potential as inhibitors is hindered by limitations such as cytotoxicity and thrombocytopenia [8-10]. Natural plant polyphenols have demonstrated effectiveness as inhibitors of antiapoptotic proteins; however, their therapeutic potential has been hindered by dose-dependent toxicity observed during clinical trials [10]. Venetoclax is the first U.S. Food and Drug Administration (FDA)-approved BH3 mimetic, indicated for treating chronic lymphocytic leukemia or small lymphocytic lymphoma [11]. Nonetheless, Venetoclax is inefficient with malignancies that show Bcl-2 Gly101Val mutation [12]. Hence, numerous efforts are underway to develop BH3-mimetics use in monotherapy or combinatorial therapy as potential Bcl-2 inhibitors.

Molecular docking and molecular dynamics simulations were used to investigate the BH3-mimetic activity of five polyphenolic compounds, known for their antiproliferative activity and their capability to downregulate Bcl-2 proteins [13-16]. The chemical structures of five polyphenolic compounds: Hesperetin ($C_{16}H_{14}O_6$), Quercetin ($C_{15}H_{10}O_7$), Cleomiscosin B ($C_{20}H_{18}O_8$), 5'-Methoxy-7'-epi-jatrorin A ($C_{20}H_{18}O_9$), and Procyanidin B2 ($C_{30}H_{26}O_{12}$), are presented in Fig.1.

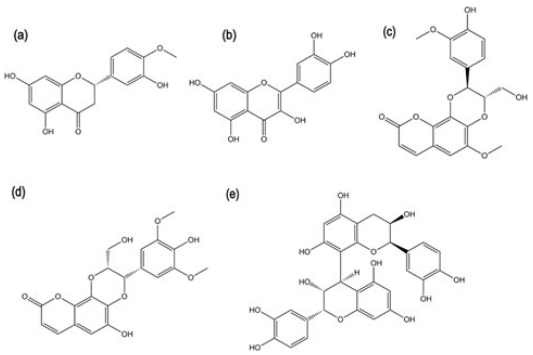

Fig. 1. Chemical structures of (a) Hesperetin, (b) Quercetin, (c) Cleomiscosin B, (d) 5'-methoxy-7'-epi-jatrorin A, and (e) Procyanidin B2.

We hypothesized that the bioactive compounds could bind within the BH3 binding pocket of either Bcl-2 wild-type (WT) or Gly101Val (G101V) mutated Bcl-2 and could act as BH3-mimetics. Molecular docking studies were employed to obtain the binding energy and investigate the structural interactions between five polyphenolic compounds inside the BH3 binding pocket

of wild-type and mutant Bcl-2 proteins. The complex structures of the bioactive compound with the maximum binding affinity to the Bcl-2 protein in molecular docking calculations are further evaluated for conformation dynamics through molecular dynamics (MD) simulations.

2. Materials and Methods

2.1 Molecular constructions

Hesperetin (Compound CID 72281), Quercetin (Compound CID 5280343), Cleomiscosin B (Compound CID 156875), and Procyanidin B2 (Compound CID 122738) were extracted from the PubChem database. The compound 5'-methoxy-7'-epi-jatrorin A was constructed and its energy was minimized using Chem3D 16.0 via the MM2 method. Molecule structures of Bcl-2 proteins from Birkinshaw's group [12] (PDB ID: 6O0K and 6O0L) and the Venetoclax molecule were selected for further molecular docking calculations as Bcl-2 WT and mutant type (Bcl-2 G101V), respectively.

2.2 Molecular docking calculations

Based on the literature and FDA-approved BH3-mimetics, the amino acid residues involved in the binding site on the Bcl-2 protein were determined. Hydrogen atoms were added, and water molecules were removed from the crystal structures via the Discovery Studio 2020 Client (DSC) program [17]. Ligands were docked into the binding site of both the WT and mutant Bcl-2 using AutoDock Tools 1.5.7 [18] and AutoDock 4.2 software packages [19]. The Bcl-2 receptor proteins were kept rigid, while ligands were kept flexible. The ligand binding pocket was centered in a grid of size 66 × 66 × 66 with a 0.375 Å spacing. The conformational search was performed using the Lamarckian Genetic Algorithm [20], with the remaining parameters set to default. One hundred docking simulations were conducted for each ligand. The best-fitting conformation, characterized by the lowest binding energy (ΔG) and a higher cluster frequency, was selected for further analysis.

2.3 Molecular dynamics simulations

MD simulations of the Bcl-2 WT and mutant Bcl-2 complexes with Procyanidin B2 were performed using the AMBER20 program package [21]. The molecular docking calculations obtained the initial coordinates of the receptor-ligand complex structures. Both receptor-ligand complexes were then placed in a periodically truncated octahedral box with TIP3P water molecules, chosen for its versatility and well-parameterized properties across a wide range of biomolecular force fields [22]. The buffer distance between the receptor-ligand complex and the box boundaries was set to 10 Å to prevent atomic migration of the complex structure to the adjacent periodic box. The recently developed AMBER-FB15 force field [23] was adopted to simulate the dynamics of Bcl-2, while the general AMBER force field was used for Procyanidin B2. The isothermal-isobaric ensemble (NPT) was employed to regulate the system environment under ambient conditions (1 atm and 25 °C).

The SHAKE algorithm [24] was applied to provide constraints for bonds connected to hydrogen atoms. MD trajectories were collected, and the stability of the receptor-ligand complex was assessed by observing system energies and the atomic root-mean-squared deviation (RMSD) for both the receptor and ligand. The binding energies between Procyanidin B2 and Bcl-2 were determined using the Generalized Born surface area continuum solvation (MM/GBSA) method [25].

3. Results and Discussion

3.1 Molecular docking validation

Re-docking is a method utilized to validate the docking protocol by employing a known crystallographic complex with a ligand. In the case of the Venetoclax molecule, the co-crystallized ligands were

removed from the protein and subsequently re-docked into their crystallographic complex using molecular docking approaches. The energy and RMSD of the binding pose were considered when validating the docking protocol. Following the re-docking process, the docked ligands were superimposed onto the crystal structures, as illustrated in Fig. 2.

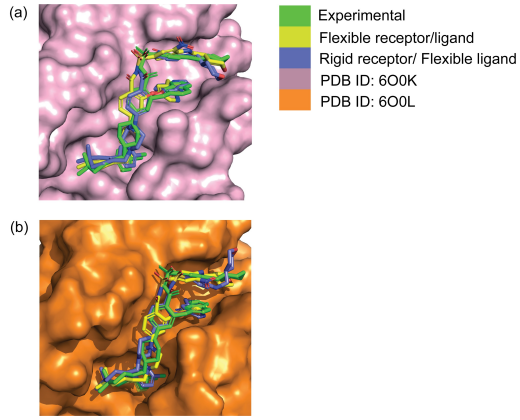

Fig. 2. The molecular superposition models of redock ligands from molecular docking. The ligands are shown in stick models, and protein structures are represented as surface.

Re-docking of Veneotoclax:6O0K and Venetoclax: 6O0L were well performed for the prediction of ΔG of bound complexes with small alterations from the experimental values around 0.72-1.84 kcal/mol and 0.32-2.32 kcal/mol for rigid and flexible docking calculations, respectively, as shown in Table **1**. As well, the results demonstrate a high similarity between the re-docked binding pose and the experimental configuration of the protein-ligand complex, with RMSD values of 1.69 Å and 1.34 Å for WT and mutated G101V, respectively. The RMSD is lower than 2.0 Å, suggesting good accuracy in the docking calculations [26]. Hence, this methodology was employed to predict the binding interactions of five polyphenolic compounds with Bcl-2 proteins.

3.2 Molecular Docking Analysis

The experimental binding energy (ΔG) values of Venetoclax are -14.58 kcal/mol with for WT and -11.58 kcal/mol for G101V [12], indicating a lower binding affinity of Venetoclax when the Bcl-2 G101V mutation occurs. This observation is consistent with our docking calculations, as depicted in Table **2**.

Table 1. The RMSD (Å) of molecular superposition between molecular docking structures and x-ray structures.

PDB ID	ΔG (kcal/mol)			RMSD (Å)			
				Rigid	Flexible		
	Exp.	Rigid	Flexible	Ligand	Ligand	Protein	Overall
6O0K	-14.58	-12.74	-14.90	1.61	1.69	0.68	1.48
6O0L	-11.58	-12.30	-13.90	1.84	1.34	0.52	1.19

The docking calculations for ΔG values of Quercetin and 5'-methoxy-7'-epi-jatrorin A compounds show lower binding affinity with the mutated G101V Bcl-2, similar to Venetoclax. The experimental binding energy of Quercetin is -7.88 kcal/mol [14] for WT, with a 0.18 kcal/mol energy difference, further validating our docking protocol.

However, Hesperetin, Cleomiscosin B, and Procyanidin B2 exhibit better binding affinity with the mutated Bcl-2 G101V, as indicated by more negative ΔG values. The ΔG value of Venetoclax is much lower than that of the polyphenolic compounds, attributed to the larger molecular size of Venetoclax compared to the five polyphenolic compounds in this study. This allows Venetoclax to occupy more volume inside the binding pocket of Bcl-2, resulting in the lower ΔG value.

Table 2. Molecular docking binding energy (ΔG in kcal/mol)) and cluster frequency between ligands and Bcl-2 proteins.

Ligands	WT	Cluster frequency	G101V	Cluster frequency
Venetoclax	-14.90	16	-13.90	4
Hesperetin	-7.50	42	-7.70	4
Quercetin	-7.70	21	-7.60	84
Cleomiscosin B	-7.30	35	-8.10	12
5'-methoxy-7'-epi-jatrorin A	-8.30	7	-7.40	29
Procyanidin B2	-8.30	6	-8.80	37

Protein-ligand interaction analysis of Venetoclax and other ligands revealed 13 common amino acid residues binding motifs of BH3 mimetics, namely A100, D103, F104, F112, M115, L137, N143, G145, R146, V148, A149, V156, and W202. Additionally, two amino acid residues, R107 and V133, were observed to interact with ligands in mutated Bcl-2.

From the molecular docking results, the five investigated polyphenolic compounds demonstrated the ability to bind to the hydrophobic cleft of the Bcl-2 protein. These findings align with in vitro analyses of Hesperetin, Quercetin, and Procyanidin B2 on various cancer cells, where they have been reported to reduce the expression of antiapoptotic proteins [15, 16]. Consequently, it can be inferred that these bioactive compounds exhibit BH3 mimetic activity. However, this activity is not as robust as that of the clinically available drug Venetoclax. Procyanidin B2 (ProB2) had the lowest ΔG of -8.30 and -8.80 kcal/mol with 6 and 37 cluster frequencies for WT and mutated Bcl-2, respectively (Table 2), indicating good binding potential. Hence, the stability of the complex structures and the conformational dynamics of ProB2/Bcl-2 complexes in an aqueous system were further analyzed by MD simulations.

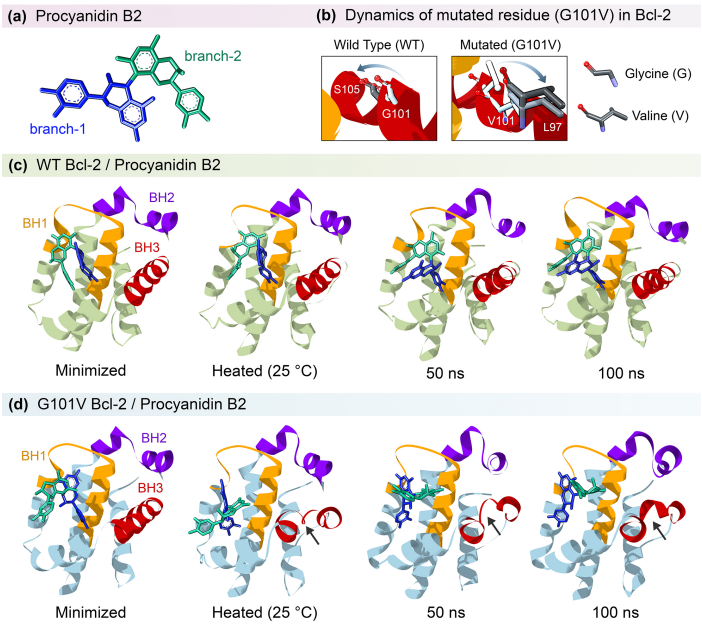

Fig. 3. The visualization of ProB2 complexed with Bcl-2 WT and G101V mutated Bcl-2 from minimization step through 100 ns MD simulations.

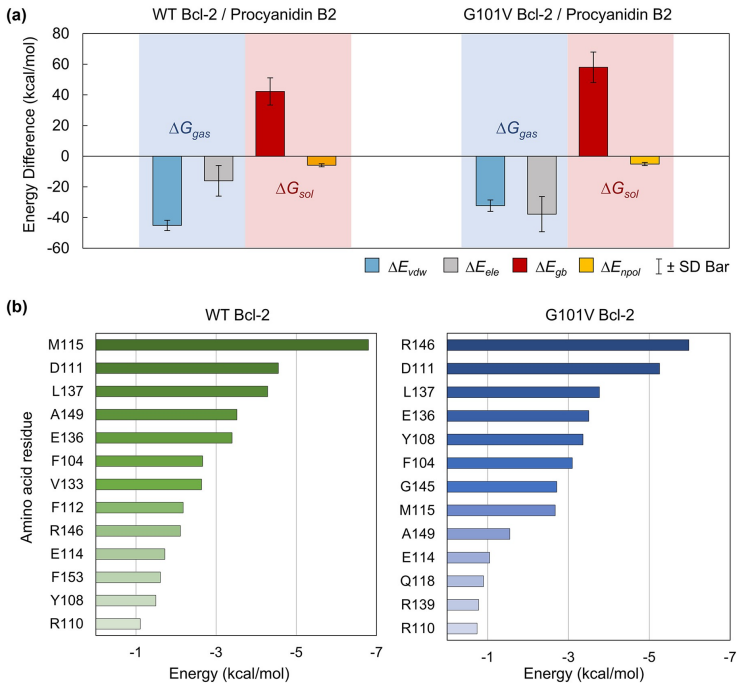

Fig. 4. Energetic contributions of binding energy for WT and mutated G101V Bcl-2/ProB2 complexes from stable interval of 90 to 100 ns.

3.3 MD Simulations Analysis

The visualization of the ProB2 complex with both Bcl-2 WT and mutated Bcl-2 G101V, spanning from the minimization step through a 100 ns MD simulation, is shown in **Fig.3**. ProB2's alias setting, represented by different colors in the stick model, distinguishes its structure. Specifically, the blue and green colors denote 'branch-1' and 'branch-2' of ProB2, respectively. The dynamic motion of the mutated amino acid residue is compared with the original residue in Bcl-2 WT. Stick models of glycine 101 and valine 101 are presented, with the carbon atoms transitioning from white to dark grey to illustrate the motion along the simulation progress (minimized to 100 ns). Stick models of both amino acid structures are displayed on the right side, excluding the hydroxyl group of carboxylic acid, as the peptide bond between amino acids forms via dehydration, resulting in the detachment of the hydroxyl group. Black arrows point to the unfolded alpha-helix in the mutated BH3 motif. All stick models are presented without hydrogen atoms for clearer visualization.

The binding affinities of ProB2 to Bcl-2 WT and mutated Bcl-2 were determined through binding free energy calculations using the MM/GBSA method. The calculations were based on 5,000 frames from the selected stable interval of 90 to 100 ns. Energetic contributions in the gas and aqueous phases are plotted in Fig. 4a. The van der Waals (ΔE_{vdw}) and electrostatic (ΔE_{ele}) energies, whose summation contributes to the energy difference in the gas phase (ΔG_{gas}), are presented as light blue and light gray bars, respectively. The electrostatic (ΔE_{gb}) and nonpolar (ΔE_{npol}) energies, whose summation contributes to solvation free energy (ΔG_{sol}), are presented as red and mustard yellow bars, respectively. Binding energy decomposition, revealing promising interacting amino acid residues, is illustrated in Fig. 4b. The interacted amino acid

residues (one-letter abbreviations) are listed on the y-axis label of bar plots, and their corresponding energies based on binding with ProB2 are shown on the x-axis. The binding strength is represented by the shade of the bar color, with strong binding presented as a darker shade and weak binding as a lighter shade.

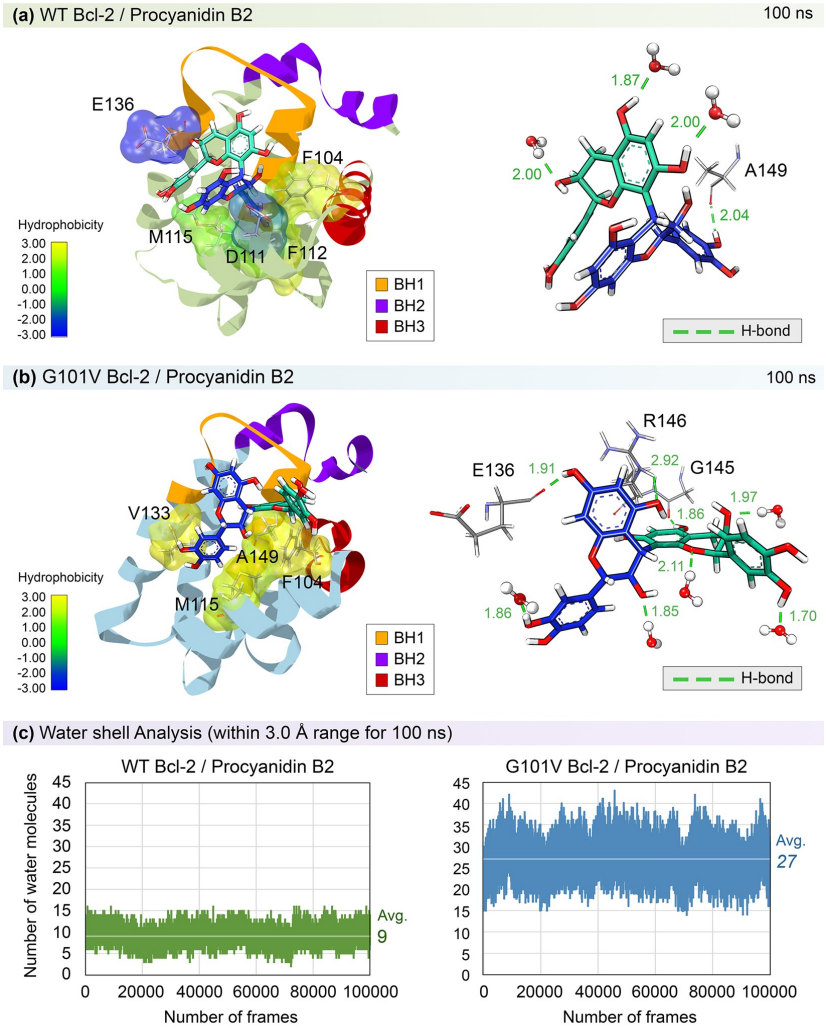

Fig. 5. The binding modes visualization and 3.0 Å water shell analysis of ProB2 with WT and mutated G101V Bcl-2.

Table 3. MM/GBSA energies (in kcal/mol) of WT and mutated G101V Bcl-2/ProB2 complexes.

Component	WT	G101V
ΔG_{gas}	-61.13 ± 9.76	-70.02 ± 11.17
ΔG_{sol}	36.34 ± 8.73	52.88 ± 9.68
ΔG	-24.79 ± 3.11	-17.15 ± 3.43

The final binding energies and major energetic components are also summarized in Table 3. The highly negative interaction energy in the gas phase (ΔG_{gas}) counteracted the positive solvation free energies (ΔG_{sol}) for both complex systems. Consequently, the total energy difference (ΔG) for both systems turned out to be negative, implying favorable protein-ligand binding. However,

the binding between ProB2 and Bcl-2 WT exhibited higher strength than the binding with the mutated species, contrary to the calculations from the molecular docking. This inconsistency may be attributed to the influence of water molecules, resulting in a different dynamic of the protein structure in a solvated environment. As discussed earlier through MD snapshots visualization, the structure of the mutated Bcl-2 displayed higher dynamic motion than the WT species, as well as the dynamics of the bound ProB2.

The binding modes and intermolecular interactions are crucial for gaining insight into the factors promoting apoptosis-inducing agents' binding. Thus, here, we focus on the analysis of binding modes of ProB2 within the hydrophobic cleft of Bcl-2. Apoptosis can be induced when the hydrophobic cavity is occupied, generally by BH3-only proteins or developed BH3-mimetics. However, the hydrophobic cavity of Bcl-2 is generally wide and shallow, posing a challenge to promote strong binding with BH3-mimetics [27]. Hence, different designs of BH3-mimetics may lead to different binding modes.

As illustrated in Fig. 5(a)-(b), the analysis is based on the MD snapshot at 100 ns, which represents the last frame of the MD production and signifies the final binding state. We found that the overall binding sites promoting the interaction with ProB2 for both WT and mutated Bcl-2 shared several amino acid residues: F104, M115, E136, and A149.

For the hydrophobic sites of Bcl-2 WT, five critical amino acid residues are labeled in Fig. 5a (left), four highly hydrophobic—F104, D111, F112, and M115. Consequently, they facilitate hydrophobic interactions with branch-1 of ProB2. While E136 exhibits less hydrophobicity, it promotes electrostatic attraction to branch-2 of ProB2. Regarding hydrogen bonding sites of Bcl-2 WT, one amino acid residue, A149, is involved, along with three water molecules, as shown in Fig. 5a (right). In contrast, the hydrogen bonding sites for mutated Bcl-2 form stronger networks involving three amino acid residues and five water molecules, as illustrated in Fig. 5b (right). Two strong hydrogen bonds are formed with E136 and G145, while a weaker hydrogen bond is formed with R146. For the hydrophobic sites of mutated Bcl-2, only four amino acids are included—F104, M115, V133, and A149—as labeled in Fig. 5b (left). As all these amino acid residues exhibit high hydrophobicity, they promote hydrophobic interactions with both branch-1 and branch-2 of ProB2. Once again, this confirms our prior analysis that the hydrophobic interaction is the dominant interaction between ProB2 and Bcl-2 WT, while the electrostatic interaction is dominant between ProB2 and mutated Bcl-2.

In order to systematically define binding pockets for Procyanidin B2 within hydrophobic cleft of Bcl-2, the reference name and definition of binding pocket should be canonical. According to Denis et al. [28], they have proposed four binding pockets (P1, P2, P3, and P4) defined by amino acid residues within 4 Å radius around Venetoclax which bound to Bcl-2 (PDB ID: 6O0K). The P1 pocket consist of Glu118 (E118), Leu119 (L119), and Arg129 (R129). The P2 pocket compose of Asp111 (D111), Phe112 (F112), Met115 (M115), Val133 (V133), Glu136 (E136), Leu137 (L137), Ala148 (A148), Glue152 (E152), Phe153 (F153), Val156 (V156). The P3 pocket consists of Phe104 (F104) and Tyr108 (Y108). The P4 pocket compose of Phe98 (F98), Ala100 (A100), Asp103 (D103), Trp144 (W144), Gly145 (G145), Val148 (V148), and Tyr202 (Y202). Therefore, Procyanidin B2 interacted with P2 and P3 pockets of wild type Bcl-2. However, it interacted with P2, P3, and P4 pockets of mutated Bcl-2. These can imply the potential of the bioactive compound as

BH3 mimetics based on the ability to occupy similar binding sites as Venetoclax. The water shell analysis around ProB2 for both WT and mutated Bcl-2 is shown in Fig. 5c. The number of water molecules found within a 3 Å spherical radius around ProB2, bound to Bcl-2 WT, is three times fewer than in the mutated Bcl-2 throughout the 100 ns simulation. The hydrophobic cleft of mutated Bcl-2 is wider than in the WT species because more water molecules can migrate into the cleft, forming interactions with ProB2. Previously, we proposed that the possible cause of the alpha-helical collapse in the mutated BH3 motif could be linked to the dynamics of the mutated residue (G101V). Thus, the widening of the mutated hydrophobic cavity could be one of the related consequences of the distorted BH3 motif. However, other underlying causes might be contributing to the widening of the mutated hydrophobic groove that are worth further investigation.

4. Conclusions

The theoretical investigation of the molecular binding of five polyphenolic compounds with both WT and mutated Bcl-2 demonstrates that these compounds can bind to the hydrophobic groove of BH3 motifs, functioning as BH3-mimetics. ProB2 exhibits satisfactory binding free energies (-8.30 to -8.80 kcal/mol) toward both WT and mutated Bcl-2 following the docking calculations. MD analysis was performed to further explore the dynamics of ProB2 when bound to the Bcl-2 protein in a solution. ProB2 shows a superior ability to tightly bind to the hydrophobic groove of WT Bcl-2 (-24.79 kcal/mol) compared to the mutated species (-17.15 kcal/mol). This is because the mutated residues in BH3 motifs significantly induce structural changes in the targeted hydrophobic cleft. Consequently, the hydrophobic cavity widens, making it more susceptible to interference by surrounding water molecules and ultimately weakening the protein-ligand interaction. The results indicate that ProB2 can be considered a promising natural BH3-mimetic due to its mechanism of action, occupying the binding site of Bcl-2, similar to Venetoclax, a commercial BH3-mimetic.

Acknowledgements

This work was supported by the Thammasat University Research Fund, Contract No. TUFT 84/2566. The author, Ayomi Vidana Pathiranage, gratefully acknowledges the financial support received from the Excellent Foreign Students (EFS) scholarship program of Sirindhorn International Institute of Technology (SIIT), Thammasat University.

References

[1] Ferlay J, Colombet M, Soerjomataram I, Parkin DM, Piñeros M, Znaor A, et al. Cancer statistics for the year 2020: An overview. International Journal of Cancer. 2021;149(4):778-89.

[2] Sung H, Ferlay J, Siegel RL, Laversanne M, Soerjomataram I, Jemal A, et al. Global Cancer Statistics 2020: GLOBOCAN Estimates of Incidence and Mortality Worldwide for 36 Cancers in 185 Countries. CA: A Cancer Journal for Clinicians. 2021;71(3):209-49.

[3] Pfeffer CM, Singh ATK. Apoptosis: A Target for Anticancer Therapy. International Journal of Molecular Sciences. 2018;19(2):448.

[4] Kale J, Osterlund EJ, Andrews DW. BCL-2 family proteins: changing partners in the dance towards death. Cell Death Differ. 2018;25(1):65-80.

[5] Campbell KJ, Tait SWG. Targeting BCL-2 regulated apoptosis in cancer. Open Biology. 2018;8(5):180002.

[6] Sharma A, Boise L, Shanmugam M. Cancer Metabolism and the Evasion of Apoptotic Cell Death. Cancers. 2019;11:1144.

[7] Chonghaile TN, Letai A. Mimicking the BH3 domain to kill cancer cells. Oncogene. 2008;27(1):S149-S57.

[8] Oltersdorf T, Elmore SW, Shoemaker AR, Armstrong RC, Augeri DJ, Belli BA, et al. An inhibitor of Bcl-2 family proteins induces regression of solid tumours. Nature. 2005;435(7042):677-81.

[9] Tse C, Shoemaker AR, Adickes J, Anderson MG, Chen J, Jin S, et al. ABT-263: A Potent and Orally Bioavailable Bcl-2 Family Inhibitor. Cancer Research. 2008;68(9):3421-8.

[10] Suvarna V, Singh V, Murahari M. Current overview on the clinical update of Bcl-2 anti-apoptotic inhibitors for cancer therapy. European Journal of Pharmacology. 2019;862:172655.

[11] Souers AJ, Leverson JD, Boghaert ER, Ackler SL, Catron ND, Chen J, et al. ABT-199, a potent and selective BCL-2 inhibitor, achieves antitumor activity while sparing platelets. Nat Med. 2013;19(2):202-8.

[12] Birkinshaw RW, Gong J-n, Luo CS, Lio D, White CA, Anderson MA, et al. Structures of BCL-2 in complex with venetoclax reveal the molecular basis of resistance mutations. Nature Communications. 2019;10(1):2385.

[13] Ferreira de Oliveira JMP, Santos C, Fernandes E. Therapeutic potential of hesperidin and its aglycone hesperetin: Cell cycle regulation and apoptosis induction in cancer models. Phytomedicine. 2020;73:152887.

[14] Primikyri A, Chatziathanasiadou MV, Karali E, Kostaras E, Mantzaris MD, Hatzimichael E, et al. Direct binding of Bcl-2 family proteins by quercetin triggers its pro-apoptotic activity. ACS Chem Biol. 2014;9(12):2737-41.

[15] Lee Y. Cancer Chemopreventive Potential of Procyanidin. Toxicological Research. 2017;33(4):273-82.

[16] Omid G. Cytotoxicity and Apoptosis Induction by Coumarins in CLL. In: Tülay Aşkin Ç, editor. Cytotoxicity. Rijeka: IntechOpen; 2018.Ch. 6. p. 90-114.

[17] BIOVIA DS. Discovery Studio Visualizer 2020 [Available from: https://discover.3ds.com/discovery-studio-visualizer-download.

[18] Morris GM, Huey R, Lindstrom W, Sanner MF, Belew RK, Goodsell DS, et al. AutoDock4 and AutoDockTools4: Automated docking with selective receptor flexibility. J Comput Chem. 2009;30(16):2785-91.

[19] Cosconati S, Forli S, Perryman AL, Harris R, Goodsell DS, Olson AJ. Virtual screening with AutoDock: theory and practice. Expert Opinion on Drug Discovery. 2010;5(6):597-607.

[20] Morris GM, Goodsell DS, Halliday RS, Huey R, Hart WE, Belew RK, et al. Automated docking using a Lamarckian genetic algorithm and an empirical binding free energy function. Journal of Computational Chemistry. 1998;19(14):1639-62.

[21] Case D, Aktulga, H.M., Belfon, K., Ben-Shalom, I., Brozell, S., Cerutti, D., Cheatham T., Cruzeiro V., Darden T., Duke R., Giambasu G., Gilson M., Gohlke H., Götz A., Harris R., Izadi S., Izmailov S., Jin C., Kasavajhala K., & Kollman, P. Amber 2021. (2021).

[22] Linse J-B, Hub JS. Three- and four-site models for heavy water: SPC/E-HW, TIP3P-HW, and TIP4P/2005-HW. The Journal of Chemical Physics. 2021;154(19).

[23] Wang LP, McKiernan KA, Gomes J, Beauchamp KA, Head-Gordon T, Rice JE, et al. Building a More Predictive Protein Force Field: A Systematic and Reproducible Route to AMBER-FB15. J Phys Chem B. 2017;121(16):4023-39.

[24] Ryckaert J-P, Ciccotti G, Berendsen HJC. Numerical integration of the cartesian equations of motion of a system with constraints: molecular dynamics of n-alkanes. Journal of Computational Physics. 1977;23(3):327-41.

[25] Genheden S, Ryde U. The MM/PBSA and MM/GBSA methods to estimate ligand-binding affinities. Expert Opin Drug Discov. 2015;10(5):449-61.

[26] Ramírez D, Caballero J. Is It Reliable to Take the Molecular Docking Top Scoring Position as the Best Solution without Considering Available Structural Data? Molecules. 2018;23(5):1038.

[27] Cory S, Roberts AW, Colman PM, Adams JM. Targeting BCL-2-like Proteins to Kill Cancer Cells. Trends Cancer. 2016;2(8):443-60.

[28] Denis C, Sopková-de Oliveira Santos J, Bureau R, Voisin-Chiret AS. Hot-Spots of Mcl-1 Protein. Journal of Medicinal Chemistry. 2020;63(3):928-43.